Chemosphere 295 (2022) 133936

Contents lists available at ScienceDirect

Chemosphere

journal homepage: www.elsevier.com/locate/chemosphere

Successful sulphide-driven partial denitrification: Efficiency, stability and resilience in SRT-controlled conditions☆

Cecilia Polizzi [a,*], David Gabriel [b], Giulio Munz [a]

[a] Department of Civil and Environmental Engineering, University of Florence, Via di S. Marta, 3, 50139, Firenze, Italy
[b] GENOCOV Research Group, Department of Chemical, Biological and Environmental Engineering, Escola D'Enginyeria, Universitat Autònoma de Barcelona, 08193, Bellaterra, Spain

HIGHLIGHTS

- Highly efficient and stable nitrite accumulation was achieved.
- Influent S/N < 0.6 g/g allowed for complete inhibition of N_2 production.
- *Thiobacillus* outcompeted *Sulfurimonas* under strict S-limiting conditions.
- Nitrate uptake rate was not affected by high nitrite levels.

GRAPHICAL ABSTRACT

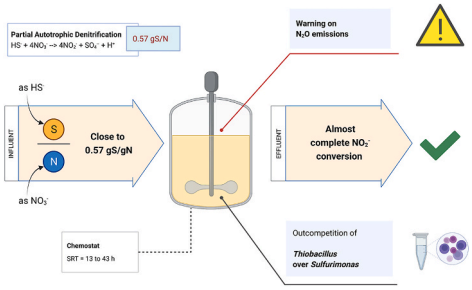

ARTICLE INFO

Handling Editor: A Adalberto Noyola

Keywords:
Sulphide-driven Partial Autotrophic Denitrification (PAD)
Nitrite accumulation
Sulphur oxidizing biomass (SOB)
Influent S/N

ABSTRACT

Partial denitrification is emerging as a valuable solution for NO_2^- supply in Anammox systems. When reduced sulphur compounds are used as electron donors, S-driven Partial Autotrophic Denitrification (PAD) can also be achieved, allowing for an integrated autotrophic nitrogen (N) and sulphur (S) removal from liquid and gaseous streams. The aim of the present work was to maximise NO_3^- reduction to NO_2^- coupled with complete HS^- oxidation, by the selective control of influent S/N ratio and sludge retention time (SRT). A 2.5-L chemostat was operated for 115 days and three operational phases were tested at decreasing SRT of 40, 23 and 13 h, testing S/N ratios in the range of 0.5–1 gS/gN. Successful sulphide-driven PAD was achieved and lead to average NO_2^- conversion efficiencies as high as77±17% at all the conditions tested, with the highest value of 99% at the lowest S/N of 0.58 gS/gN and SRT of 23 h. Respirometric tests showed that NO_3^- uptake rate was stable at 90±10 mgN/gVSS/h, when NO_3^- was present as sole electron acceptor or at NO_2^- levels as high as 120 mgN/l; on the contrary, NO_2^- uptake rates were very sensitive to the applied conditions. Metabarcoding analyses revealed that the microbial community was highly enriched in Sulphur Oxidizing Bacteria (SOB>80%) and stable S-limiting conditions appeared to favour *Thiobacillus* over *Sulfurimonas* genus. A preliminary assessment of N_2O potential emission was also performed. To the best of our knowledge, this is the first work evaluating the synergic effect of SRT and influent S/N ratio on nitrite accumulation in highly SOB-enriched systems and the NO_2^- conversion efficiencies achieved are among the highest reported in literature.

☆ All the authors contributed to the revision of the work and agreed with the final version of the article.

* Corresponding author. Via di S. Marta, 3, 50139, Firenze, Italy.
E-mail address: cecilia.polizzi@unifi.it (C. Polizzi).

https://doi.org/10.1016/j.chemosphere.2022.133936
Received 30 September 2021; Received in revised form 30 December 2021; Accepted 7 February 2022
Available online 8 February 2022

1. Introduction

The anammox process has been conventionally combined with Partial Nitritation (PN) as their synergy allows for a significant reduction in oxygen requirement and sludge production compared with conventional nitrification-denitrification systems. Nevertheless, PN long-term stability is challenged by the successful and stable suppression of nitrite oxidizing bacteria (NOB) and partial denitrification is emerging as an alternative route for nitrite supply in anammox systems (Zhang et al., 2019). In case reduced sulphur compounds (such as sulphide, thiosulphate or sulphur) are used as electron donors, Partial Autotrophic Denitrification (PAD) can also be achieved. Some industrial wastewaters from chemical and food processing as well as petroleum and leather processing are highly rich in nitrogen (N) and sulphur (S) compounds, the latter being present also in gaseous streams, typically in the form of hydrogen sulphide (Cristovao et al., 2015; Jain et al., 2020; Mannucci et al., 2010). Thereby, the combination of PAD and Anammox (PAD/A) appears particularly appealing for an integrated S and N removal through anaerobic and autotrophic processes, offering a sustainable alternative also for sulphide-rich gaseous streams such as biogas. Despite the fact that the link between sulphur-based denitrification and anammox lays at the very beginning of the anammox story (Mulder et al., 1995), little attention has been paid on the feasibility of achieving stable nitrite accumulation over sulphide oxidation as a possible pre-treatment for anammox (Chen et al., 2018; Liu et al., 2017). Recently, higher attention has been devoted to the one-stage PAD/A. Successful one-stage PAD/A operation are reported by Chen et al. (2018), Deng et al. (2021) and Kalyuzhnyi et al. (2006), among others. The promising results show the key role of influent S/N ratio, short hydraulic retention time (HRT) and high loading rates (the latter two often linked). When sulphide is used as electron (e−) donor in simultaneous PAD/A, its potential toxicity on the anammox biomass should be properly assessed, since IC_{50} are reported in the range of 0.1–5 mgS/l (Dapena-mora et al., 2007; Russ et al., 2014). A two-stage process could provide stable and controlled nitrite accumulation through partial autotrophic denitrification for a subsequent anammox treatment, limiting the risk of (irreversible) sulphide toxicity (Huang et al., 2021). Colourless Sulphur Oxidizing Bacteria (SOB) are a wide group of bacteria capable of using reduced forms of sulphur as e−donors and oxygen or nitrate/nitrite as terminal e−acceptors. Even though the metabolic pathways proposed for sulphide oxidation are quite complex (Ghosh and Dam, 2009), its oxidation to sulphate is typically considered as a two-step process, elemental sulphur (S^0) being the intermediate product. Autotrophic denitrification, i.e. SOB anoxic respiration, follows the 4-step reduction chain (NO_3^-→ NO_2^-→ NO→ N_2O→ N_2), but nitrite is typically considered the main intermediate, in a two-step denitrification assumption. The catabolic reactions of denitratation (NO_3^-→ NO_2^-) and denitritation (NO_2^-→ N_2) coupled with complete or partial sulphide oxidation are presented in the following equations:

$$HS^- + 1.6NO_3^- + 0.6H^+ \rightarrow SO_4^{2-} + 0.8N_2 + 0.8H_2O \quad \Delta G = -744.4\ Kj/molS \tag{1}$$

$$HS^- + 4NO_3^- \rightarrow SO_4^{2-} + 4NO_2^- + H^+ \quad \Delta G = -480.2\ Kj/molS \tag{2}$$

$$HS^- + 0.4NO_3^- + 1.4H^+ \rightarrow S^0 + 0.2N_2 + 1.2H_2O \quad \Delta G = -196.4\ Kj/molS \tag{3}$$

$$HS^- + NO_3^- + H^+ \rightarrow S^0 + 0.2NO_2^- + H_2O \quad \Delta G = -130.3\ Kj/molS \tag{4}$$

The multiple intermediate steps occurring both in the oxidation and reduction reactions and the high chemical reactivity of sulphide significantly increase process complexity. As a consequence, the selective control of one catabolic step over the others might be a challenging task since multiple combinations of e-donors and e-acceptors can occur. On the one hand, the application of the novel PAD/A process would be limited to wastewaters baring proper sulphide/nitrate/ammonia ratios, as required by the two processes. On the other hand, the remarkable versatility of the PAD process allows for a wide combination of S/N loads, ranging from 0.6 to 2.3 gS/gN (eqs. (2)) and (4)), widening its application to different types of wastewaters and/or gaseous streams, as above mentioned.

The selective control of the sole denitratation step is referred to as Partial Denitrification. According to equations (1) and (2), 1.43 and 0.57 gS/gN are required to drive complete sulphide oxidation coupled with complete and partial denitrification, respectively. In S-driven denitrification, nitrite accumulation is reported in continuous or batch operations as a transient or undesired consequence of e−donor limitation or overload conditions (Campos et al., 2008; Manconi et al., 2007). Nitrite can be potentially toxic for a wide range of microorganisms; there is general consensus on the fact that the actual cytotoxic role is played by its conjugated acid, the free nitrous acid, FNA (Zhou et al., 2011). Although the inhibition mechanisms on denitrifiers are not fully understood, it is often reported that the major mechanism is due to enzymatic inhibition of NO_2^- reductase, as well as on N_2O reductase, the latter being responsible for possible N_2O emissions (Wang et al., 2018; Zhou et al., 2011). Thereby, when targeting high NO_2 accumulation, high FNA concentration might favour denitritation inhibition and further nitrite accumulation. Yet, drawbacks on N_2O release must be addressed as well. To the best of our knowledge, the role of sludge retention time (SRT) in nitrite accumulation efficiency is not addressed in literature, since systems with no SRT control are often reported for PAD or PAD/A applications. Moreover, the possible role of different functional strains has been speculated by some authors, but the evidences on microbial diversity are not exhaustive to clearly depict the actual impact on process performance (Cui et al., 2019b; Moraes and Foresti, 2012).

In the present work, stable nitrite accumulation over sulphide oxidation was challenged at different influent S/N ratios and SRT values, in chemostatic conditions. Monitoring of microbial population, N_2O emissions as well as respirometric tests were performed for a more comprehensive understanding of the system response to the applied conditions.

1.1. Material and methods

1.1.1. Reactor operation

A 2.5-L glass completely stirred tank reactor (CSTR) was operated for 115 days. The reactor was seeded with SOB-enriched suspended sludge, withdrawn from a pilot-scale denitrifying CSTR treating hydrogen sulphide absorbed from biogas (source reactor conditions: Sulphide Loading Rate, SLR, up to 2.4 gS/l/d, 2000–3000 ppmv of H_2S; 1000–3000 mgN/l). Completely mixing conditions were provided by mechanical stirring (100–120 rpm) and temperature was maintained at 30±1 °C by continuously recirculating tempered water in the steel bottom jacket of the reactor. Mineral medium was prepared according to Mora et al. (2014) apart from nitrate and sulphur concentration. Nitrate was added in the mineral medium as KNO_3. A concentrate sulphide solution (0.1–0.2 M) was prepared with $Na_2S{\cdot}9H_2O$ salt, fed separately and kept in an air-tight browned bottle, connected to a N_2 gas pocket, in order to prevent air inlet and compensate inner depression caused by pump suction. The two solutions were fed in continuous by means of peristaltic pumps (Gylson Minipuls 3). A moderate flow of 0.1 l/min of a mixture of N_2–CO_2 (95% and 5%, respectively) was regulated by mass flow controllers (Low-Δp-flow mass meter, Bronkhorst) and bubbled at the bottom of the reactor in order to strip away any residual/undesired

dissolved oxygen (DO). Reactor pH was controlled by adding acid/base solutions (1 M HCl and 1 M NaOH, respectively) and set at 7.3±0.1 for the first 15 days of operation to accommodate the inoculum and then increased to 7.6±0.1. Pumps operation, temperature, pH control and flowmeters were controlled by a centralised PLC. The reactor was operated as an ideal chemostat, without biomass recirculation; thereby, SRT was directly determined by dilution rates. Regular cleaning of reactor's internal walls and submersed mechanical stirrer and tubes was performed in order to remove any possible biofilm formation that could have altered the actual SRT. As a matter of fact, biofilm formation was never relevant but cleaning operations were performed anyway as a precautionary measure.

Influent S/N was always kept below 1.43 gS/gN (eq. (1)), while a minimum of 0.57 gS/gN was ensured to provide sufficient e-donor to convert all the influent nitrate to nitrite (eq. (2)). In this work, sulphide limiting conditions are referred to influent conditions with S/N ratio below the theoretical ratio required by complete denitrification equation (eq. (1)). Slightly limiting conditions are referred to S/N values slightly below the ratio required in equation (1) and falling in the range of 0.80–1.40; strict limiting conditions are referred to S/N values close or equal to the ratio required in eq. (2), falling in the range of 0.57–0.79. Applied operational conditions are summarised in Table 1. Phase 1, 2 and 3 were planned to test decreasing SRT of 40 to 23 to 13 h and a range of S/N ratio, from slightly limiting to strictly limiting conditions for the e-donor. The first 22 days of operation (phase 1a) were characterized by highly variable influent S/N, due to technical problems mainly related to the fine tuning of the concentrated sulphide solution pump. Stable conditions were maintained from phase 1b on. SRT reduction at each phase was achieved by doubling influent flowrate; nitrate concentration in the mineral medium was kept at 200 mgN/l throughout the experimental period whereas sulphide concentration in the concentrated solution was set according to the required S/N ratio. Therefore, each phase change implied a concomitant doubling in Nitrogen Loading Rate, NLR (from 0.1 to 0.2 to 0.4 gN/l/d).

Moreover, the potential inhibition effect of high nitrite level was also addressed. FNA concentrations were calculated according to the following equation (Anthonisen et al., 1976):

$$FNA = \frac{NO_2^-}{k_a * 10^{pH}} \tag{3}$$

where $k_a = e^{\left(-\frac{2300}{273+T}\right)}$, FNA and NO_2^- are expressed as mgN/l and T as °C.

1.1.2. Process performance assessment

Nitrate removal efficiency (NRE) was expressed as the net nitrate removal between influent and effluent concentration; nitrite conversion efficiency (NiCE) as the nitrite production over the removed nitrate; nitrite accumulation efficiency (NiAE) as the nitrite production over the influent nitrate and the dinitrogen gas production efficiency (dNPE) as the gaseous nitrogen produced over the influent nitrate. The mathematical formulations for efficiencies calculations are as follows:

$$NRE = \frac{NO_3^- in - NO_3^- out}{NO_3^- in} \cdot 100 \tag{4}$$

$$NiCE = \frac{NO_2^- out}{NO_3^- in - NO_3^- out} \cdot 100 \tag{5}$$

$$NiAE = \frac{NO_2^- out}{NO_3^- in} \cdot 100 \tag{6}$$

$$dNPE = \frac{N_{2out}}{NO_3^- in} \cdot 100 \tag{7}$$

Where $NO_3^-{}_{in}$ is the nitrate concentration in the influent and $NO_3^-{}_{out}$ and $NO_2^-{}_{out}$ the nitrate and nitrite concentration in the effluent (all expressed as mgN/l).

Considering the rate of the two denitrification steps, in case of unbalance between the denitratation rate (r_dNO3) and the denitritation rate (r_dNO2), the resulting nitrite accumulation rate (r_NiA) can be calculated according to equation (8):

$$r_{NiA} = r_{dNO3} - r_{dNO2} \tag{8}$$

the rates expressed as gN/gVSS/h.

At steady-state conditions, biomass yield was calculated according to equation (9).

$$Y_{X/S} = \frac{VSS_{out} - VSS_{in}}{HS_{in}^- - HS_{out}^-} \tag{9}$$

Since the reactor was fed with synthetic wastewater along the whole experimental period, VSS_{in} was zero and VSS_{out} was the concentration measured in the CSTR.

1.1.3. Respirometric tests

The respirometric equipment and procedure described by Mora et al. (2014) were adopted. Biomass was centrifuged at 10000 rpm and concentrated approximately 4 times, by resuspension in a nutrient-free medium, except for test A, in which the reactor supernatant was used for biomass resuspension. Tests were run at day 54, 94, 102 and 113 of the CSTR operation. Pulses of concentrated solutions (1 M KNO_3, 0.5 M $NaNO_2$, 0.2–0.4 M $Na_2S{\cdot}9H_2O$) were added, according to the targeted concentrations. After each pulse, samples were taken every 10–40 min, depending on the test. TSS and VSS were analysed at the end of the test by filtering the entire liquid volume. The initial concentrations of e-acceptor and e-donor, for each test, are reported in Table 2.

Uptake rates were calculated for the N and S species by linear regression of concentrations trends observed in the test and, as a general rule, only value with $R^2 > 0.95$ were considered as reliable estimations (if not specified otherwise). For each test, two steps were distinguished: step 1 referring to sulphide consumption and step 2, for S^0 consumption. Endogenous activity was neglected in agreement to previous works

Table 2
Initial concentrations of respirometric tests.

	NO_3^- mgN/l	NO_2^- mgN/l	HS^- mgS/l	Aim of the test
Test A	85	30	20	e-acceptor competition (preliminary)
Test B	35	5	40	Maximum NUR
Test C	–	55	10	Maximum NiUR
Test D	10	120	30	NiUR and NUR at high NO_2^- concentrations

Table 1
Applied operation conditions and main results.

Phase	Days	SRT h	S/N gS/gN	NLR gN/l/d	NRE %	NiCE %	NiAE %	dNPE %
Phase 1a	1–22	44±2	1.76±1.65	0.10±0.02	76±25	7±2	5±2	72±24
Phase 1b	23–51	40±2	0.67±0.16	0.11±0.01	83±4	76±6	63±7	20±5
Phase 2	52–93	23±1	0.65±0.12	0.20±0.01	74±7	95±7	70±6	4±5
Phase 3	94–115	13±1	0.96±0.20	0.38±0.05	82±8	73±17	57±9	25±13

(Mora et al., 2014).

1.1.4. Analytical methods

Samples were filtered with 0.22 μm disposable syringe and analysed for nitrate, nitrite, sulphate and thiosulphate by ionic chromatography (Dionex ICS-2000, ThermoScientific). Sulphide was analysed with a Silver/Sulphide ion selective electrode (VWR International Eurolab, S. L). Sulphide concentration was analysed on the fresh feedstock solutions and right before replacing it with a new one; intermediate checks were also performed, if deemed necessary. Elemental sulphur was assessed according to sulphur mass balance (Mora et al., 2015). VSS and TSS were analysed once or twice a week, according to standard methods (APHA, 2005). N_2O concentration in the reactor headspace was analysed with Unisense N_2O microsensor; the sensor was placed in the headspace of the reactor and measurements recorded for 3–5 h.

1.1.5. Microbial community analysis

Biomass samples were collected at day 0 (inoculum) and at the end of each phase (days 49, 80, 114). Samples were centrifuged and concentrated multiple times. DNA was extracted with commercial kit (Norgen, Biofilm-kit), according to the manufacturer's instructions. DNA concentration and purity were checked by analyses on NanoDrop 1000

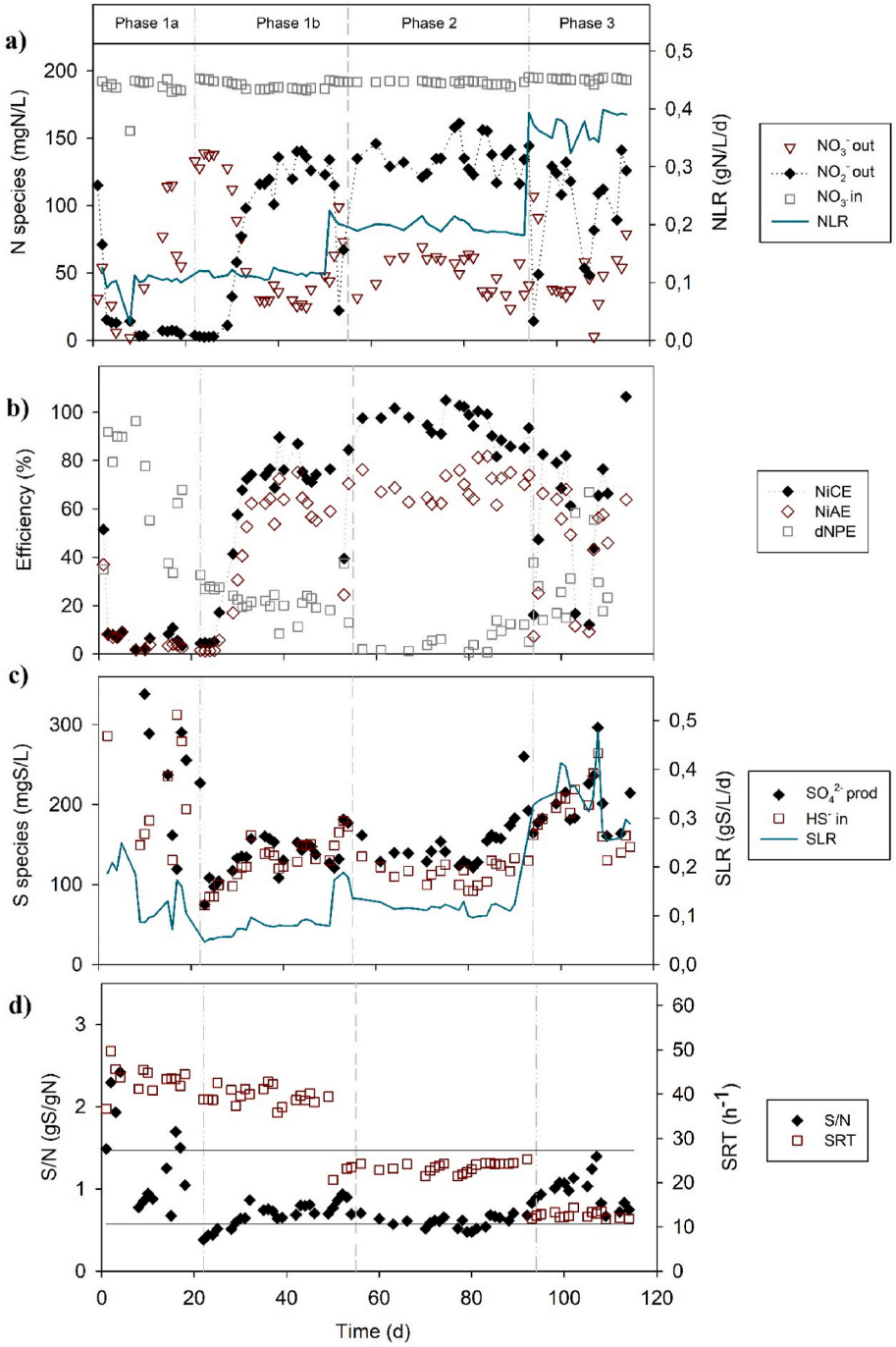

Fig. 1. Experimental results on reactor operation and performance: a) influent and effluent nitrogen concentrations; b) nitrogen conversion efficiencies; c) influent sulphide and produced sulphate concentration; d) applied SRT and S/N, horizontal continuous lines indicate S/N ratios required by equations (1) and (2). (For interpretation of the references to colour in this figure legend, the reader is referred to the Web version of this article.)

Spectrophotometer (Thermo Fisher Scientific). Extracted DNA samples were delivered to the UAB Genomics and Bioinformatic Service (Universitat Autonoma de Barcelona). PCR amplification targeted the V3 and V4 region of 16s gene and amplicon sequencing was conducted on Illumina MiSeq according to the Illumina MiSeq protocol for library preparation (support.illumina.com/content/dam/illuminasupport/documents/documentation/chemistry_documentation/16s/16s-metagenomic-library-prep-guide-15,044,223-b.pdf" title="https://support.illumina.com/content/dam/illuminasupport/documents/documentation/chemistry_documentation/16s/16s-metagenomic-library-prep-guide-15,044,223-b.pdf">https://support.illumina.com/content/dam/illuminasupport/documents/documentation/chemistry_documentation/16s/16s-metagenomic-library-prep-guide-15044223-b.pdf). Taxonomic classification was based on Greengenes database. Raw reads and taxa abundance data are available in the NCBI GEO database (accession number GSE192713).

1.2. Results and discussion

1.2.1. Successful NO_2^- accumulation

In Fig. 1, results on the reactor operation are reported. The main findings at each phase are summarised in Table 1. Since inoculum biomass was not diluted nor washed prior to inoculation, initial concentrations of nitrite, nitrate and sulphate in phase 1a were one order of magnitude higher than those achieved at steady-state conditions in the following phases, due to higher loading conditions in the source reactor.

In phase 1a, S/N ratio and nitrate removal were highly variable and no significant nitrite was observed in the effluent. In phase 1b, influent S/N was set stably within the targeted range (continuous lines in Fig. 1d), ensuring S-limiting conditions at a dilution rate of 0.025 h^{-1} (SRT of 40 h). According to the catabolic stoichiometry of equations (1) and (2), the sulphide provided in the first week of phase 1b was sufficient either to a full denitrification of 30% of the influent nitrate load or for an almost complete conversion to nitrite (assuming sulphide complete oxidation to sulphate). From day 22 to day 29, a 30% of nitrate removal efficiency was, in fact, observed and accomplished by complete conversion of nitrate to dinitrogen gas (no nitrite was detected). After a few days of stable and strict sulphide limiting conditions, a gradual nitrite accumulation was observed, until a stable effluent concentration of 125±9 mgN-NO_2^-/l was maintained, resulting in a NiAE of 63±5% and a NiCE of 76±6%. In this phase, sulphate production closed sulphur balance within a 10% error, indicating that all the influent sulphide was converted to sulphate. At day 52, SRT was halved to 23 h (phase 2). The sudden increase of loading rates and dilution rate (0.04 h^{-1}), determined a net drop in nitrite concentration down to 22 mgN-NO_2^-/l. Nevertheless, in three days, the concentration raised back to values of 136±13% mgNNO_2^-/l, kept throughout phase 2. A NiCE of 95±7% was achieved with a concomitant NiAE of 70±6%. On days 61–71, the lowest S/N of 0.58 gS/gN was maintained and resulted in the maximum and basically complete nitrite conversion with NiCE of 99±2%. Thereby, complete inhibition of dinitrogen gas production was obtained, i.e. the denitritation rate was almost zero. During phase 2, sulphate production was exceeding the influent sulphide by a 10–30%. It is assumed that thiosulphate or sulphate were present in the concentrated sulphide solution as a result of sulphide chemical oxidation. Since only 4 e−are donated per mole of S–$S_2O_3^{2-}$ oxidized to SO_4^-, compared to 8 e-mol per molS-HS^- oxidized to SO_4^{2-}, the catabolic S/N ratio required for complete or partial denitrification over thiosulphate are as high as 2.9 and 1.1 gS/gN, respectively. Thereby, in the worst case of sole thiosulphate (and not sulphate) presence, the ultimate effect on nitrogen conversion is deemed as low as 15%. In order to limit abiotic sulphide oxidation products, sulphide solution in phase 3 was prepared with freshly opened sulphide salt. In phase 3, the applied dilution rate was increased to 0.08 h^{-1} (SRT of 13 h). As in the transition from phase 1 to phase 2, the sudden flowrate and load increase lead to a drop in nitrite concentration down to 49 mgN-NO_2^-/l. Successfully, nitrite accumulation recovered within three days. In phase 3, a S/N ratio of 0.96±0.2 gS/gN was applied, in fact a value slightly higher than phase 2, and restored N_2 production, successfully inhibited in phase 2. Despite that, a satisfactory nitrite concentration of 119±15 mgN-NO_2^-/l was ensured. On day 108, a S/N ratio of 1.39 gS/gN was accidently applied. As a consequence, nitrite concentration dropped again, but high nitrite levels were restored within one day, as the S/N returned S-limited from day 109 on. Phase 3 was characterised by more unstable operational conditions, but conversion efficiencies were maintained as high as 73±17% and 57±9% for NiCE and NiAE, respectively. Sulphate production in phase 3, closed sulphur balance with a 10% error, indication that the inlet sulphide was completely oxidized to sulphate. Elemental analysis conducted on day 106 and 107 confirmed that only 2.3±0.8% of the dry matter were actually accounted as sulphur.

VSS concentration in the reactor remained very low with average concentrations of 13±5, 13±2 and 36±10 mgVSS/l, in phase 1, 2 and 3, respectively. VSS/TSS ratio remained stable at 83 ± 5%. The higher value observed in phase 3 was crossed with the elemental analysis and it did not seem to be related to significant elemental sulphur accumulation, as discussed above. Biomass yield estimated in phase 1, 2 and 3 were 0.11±0.05, 0.12±0,04 and 0.19±0.09 gVSS/gS, respectively. The observed yields are in line with the values of 0.13 gVSS/gS reported by Can-dogan et al. (2010) and lower than those reported by Campos et al. (2008) and Mora et al. (2014) ranging values of 0.33–0.36 gVSS/gS. To the best of our knowledge, none of the available yields in literature is estimated from a continuous system operating partial denitrification as the main process.

SRT as low as 12 h did not cause any biomass washout, indicating an actual biomass growth rate higher than the applied dilution rate of 0.08 h^{-1}, i.e. 1.8 d^{-1}, in line with the reported value of maximum growth rate of denitrifying SOB, ranging from 1.2 to 3 d^{-1} (Claus and Kutzner, 1985; Mora et al., 2015; Oh et al., 2000). A further increase in dilution rates is considered an interesting development of the present work, since it would allow to study both the effect of higher loading rates and the maximum biomass growth rate, at high nitrite levels.

According to the main outcomes, successful nitrite accumulation was achieved by ensuring strict sulphide-limiting conditions, i.e. S/N ratios less than 0.8 gS/gN, in SRT-controlled conditions. The closer the S/N ratio to the value of 0.57 gS/gN, required by equation (2), the higher the conversion efficiency. NiCE higher than 70% were obtained at all the SRT tested. It is speculated that SRT control contributed to system stability: the low values applied might have promoted a highly selected SOB culture, conferring the remarkable system resilience observed. Similarly to the present study, Deng et al. (2019) and Huang et al. (2021) challenged nitrite accumulation over nitrate reduction in S-driven denitrification system by maintaining S-limiting conditions, i.e. low S/N values. The maximum nitrite conversion efficiencies obtained in the mentioned studies are 50 and 55.3%, respectively, whereas an average value of 75% has been stably maintained in the present work with a maximum 99% conversion obtained at the lowest S/N ratio of 0.58 gS/gN at SRT of 23 h. Other studies report successful NO_2^- accumulation even though S/N is either not specified or significantly over stoichiometric for the e−donor (Chen et al., 2018; Liu et al., 2017), showing other possible strategies for nitrite accumulations, e.g. using S^0 instead of sulphide or high Sulphide loading rates.

1.2.2. N_2O emission and FNA role

Nitrous oxide was measured in the headspace at the end of phase 1 (days 47 and 50) and phase 2. No measurements could be performed during phase 3. A summary of the measured N_2O concentrations is available in table S1, in the supplementary material. An average concentration of 2.1±0.6 μmol/l and 3.7±0.2 μmol/l (as N_2O) was estimated for phase 1 and phase 2, respectively. Since no measurements were conducted in the liquid phase nor estimates of the k_{La} of the system were available, N_2O emissions were estimated according to mass balances over the gas phase and the derived considerations are considered

as illustrative more than exhaustive. N_2O emissions were estimated as 2.0±0.5 and 2.4% of the influent $N–NO_3^-$ load in phase 1 and phase 2, respectively. In the mini-review presented by Cui et al. (2019a), S-based autotrophic (complete) denitrification systems often exhibit lower emission factors than the heterotrophic ones, with values of 0.01–0.8% vs 2.3–13%, respectively. In the present work higher N_2O emissions were estimated. However, direct comparison of emission factors might be deceptive due to differences in mixing conditions. Differently from the reported studies adopting UASB configurations or static batch tests (Liu et al., 2016; Yang et al., 2016), continuous mixing and nitrogen gas bubbling were provided in the present work, likely promoting higher liquid-gas transfer efficiencies. Yet, the sulphide limiting strategy adopted might have promoted the production of denitrification intermediates other than nitrite. N_2O concentration increased with increasing FNA in the bulk (tab. S1). High pH are reported to be effective for N_2O emission attenuation in presence of high nitrite levels (Wang et al., 2018; Zhou et al., 2007) and might be considered for mitigation. It can be claimed that FNA inhibition was not crucial for triggering NO_2^- accumulation, but its role in maintaining stable PAD cannot be excluded. On the contrary, preliminary results warns on its possible impact in N_2O emission and further studies on pH-based mitigation strategies are recommended.

1.2.3. *Microbial diversity*

Fig. 2 reports the results on microbial diversity at class and genus level. Operational taxonomic units showing a relative abundance lower than 1% are not presented. A clear shift in SOB population was observed at class and, consistently, at genus level. At genus level, *Sulfurimonas* (ε-proteobacteria) exhibited a relative abundance of 90% in the seeding sludge whereas its relative abundance dropped to 4% and 1% on days 49 and 80, respectively, and then raised back to 53% on day 114. On the contrary, the relative abundance of *Thiobacillus* genus (β-proteobacteria) was lower than 1% in the seeding sludge, but increased to 47% on day 49 and then reached 83% on day 80, prior to decrease to 38% on day 114. Day 49 and 80 are representative of the stable and strict S-limiting conditions applied during phase 1b and 2. Day 115, on the contrary, was

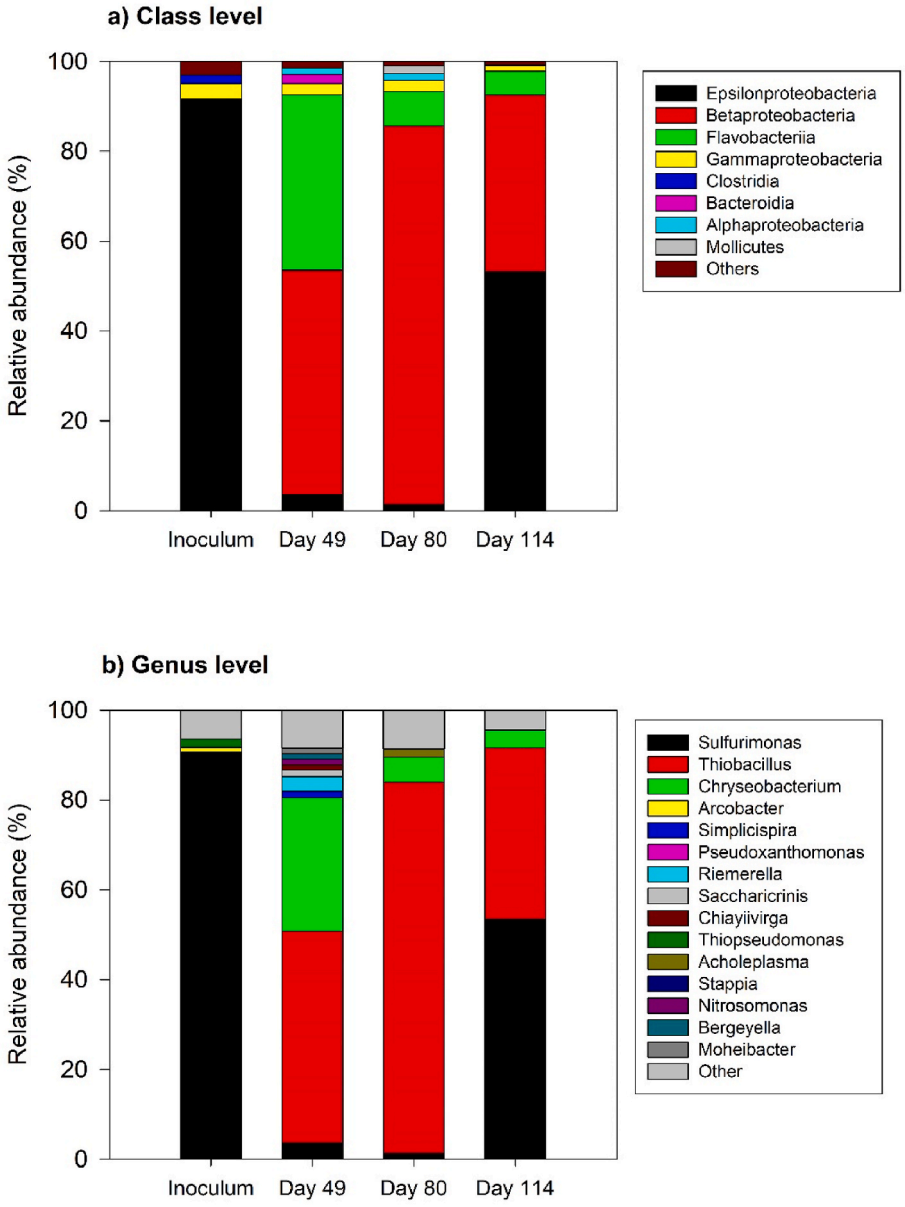

Fig. 2. Microbial diversity in the inoculum and across the three operational phases. (For interpretation of the references to colour in this figure legend, the reader is referred to the Web version of this article.)

characterised by a slightly higher S/N. Interestingly, *Thiobacillus denitrificans* has been reported to have a higher efficiency in terms of growth bioenergetics compared to *Sulfurimonas denitrificans* (Klatt and Polerecky, 2015). The proposed reasons are related to the fact that *T. denitrificans* adopts membrane-bond nitrate reductase (*Nar*) and *S. denitrificans* periplasmic nitrate reductase (*Nap*) instead. Indeed, the activity of *Nar* is directly linked to proton motive force generation as protons are driven across the cytoplasmic membrane and energy is directly harvested during its action, while *Nap* activity does not determine any direct proton motion, since its action occur directly in the periplasmic environment (Sparacino-Watkins et al., 2014). Moreover, the activity of *Nar* is less influenced by environmental conditions due to the fact that the reduction reaction occurs in the cytoplasm, differently from the *Nap* which operates in the periplasm, more susceptible to environmental conditions, such as pH (Glass and Silverstein, 1998). *Thiobacillus* is also reported to encode both the enzymatic pools required in the Sox system and in the branched pathway for S-oxidation, whereas *Sulfurimonas* only relies on the Sox system, resulting in a competitive advantage of the more versatile genus of *Thiobaicllus* (Klatt and Polerecky, 2015). It can be speculated that strict and stable energy limited conditions, resulting from e−donor limitation, lead to a competitive advantage of the genus with higher energy efficiency. The role of the periplasmic nitrite and nitrate reductases, more sensitive to environmental conditions compared to the membrane-bond nitrate reductase is considered of relevance for defining the theoretical framework behind successful PAD systems. A 30% relative abundance of *Chryseobacterium*, belonging to the class of *Flavobacterium*, was also detected on day 49. Their presence is not fully understood since these bacteria are typically reported as heterotrophic and the only organic matter available was the organic compounds deriving from endogenous decay of biomass.

The nitrite drop episodes and subsequent nitrite accumulation recovery reveal a remarkable functional resilience of the system, against daily S/N variations, and suggest that successful nitrite accumulation was not due to the selection of biomass lacking of the enzymatic pool for complete denitrification, as speculated in other studies (Chen et al., 2018; Cui et al., 2019b), since the accumulated nitrite was promptly reduced in presence of abundant electron donor. Cell-signalling mechanisms, such as Quorum Sensing (QS), are speculated to have played a role in the first catabolic shift observed on days 29–33, when complete denitrification was gradually replaced by partial denitrification, provided stable S-limiting conditions. QS molecules have been, in fact, reported to affect denitrification activity likely acting at the transcriptional level of the reduction-chain enzymes (Cheng et al., 2017).

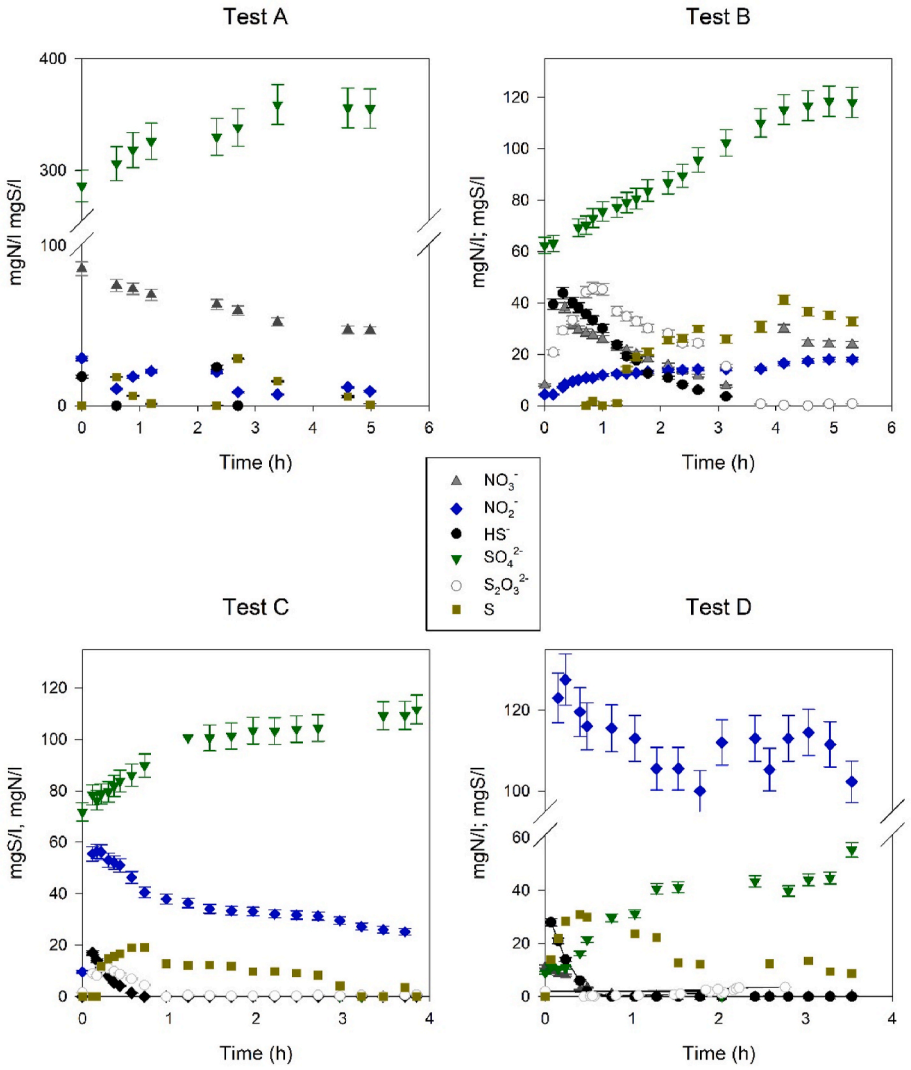

Fig. 3. Results from respirometric tests A, B, C and D. (For interpretation of the references to colour in this figure legend, the reader is referred to the Web version of this article.)

1.2.4. Respirometric tests

Results of respirometric tests are reported in Fig. 3. In test A, a preliminary NUR estimation was 100±35 mgN/gVSS/h, as an overall value in step 1 and 2, and confirmed in the subsequent tests.

In test B, thiosulphate formation was observed at the beginning of the test and it is believed to result from chemical interactions between dissolved sulphide and other chemically forms S intermediates (Van Den Bosch et al., 2007). Thiosulphate uptake is considered as representative of sulphide uptake since it is considered interchangeable with sulphide for chemolithotrophic biomass and is often used for SOB kinetic assessment (Mora, 2014). During step1, uptake rates were 80 mgN-NO_3^-/gVSS/h, 200 mgS-HS^-/gVSS/h and 125 mgS-$S_2O_3^{2-}$/gVSS/h. A small but constant accumulation of nitrite was also observed at a rate of 12 mgN-NO_2^-/gVSS/h ($R^2 = 0,94$). According to eq. (8), nitrite consumption rate resulted in 65 mgN-NO_2^-/gVSS/h. NUR uptake over S oxidation was not clearly profiled. In test C, a temporary delay in nitrite consumption was observed. It can be speculated that it could result from an enzymatic delay since biomass was grown on nitrate only and nitrite was predominantly accumulated rather than consumed. Uptake rates resulted in 190 mgN-NO_2^-/gVSS/h; 140 mgS-HS^-/gVSS/h and 90 mgS-$S_2O_3^{2-}$/gVSS/h. NiUR in step2 was as low as 27 mgN-NO_2^-/gVSS/h, 7 times lower than the value observed in step1. Test D was conducted at nitrite levels as high as those observed in the CSTR, in order to assess whether nitrite inhibition was playing a significant role in the reactor performance and the estimated FNA was 4–5 μgN/l. When sulphide was present as sole e-donor, test D exhibited the following rates: 85 mgN-NO_3^-/gVSS/h; 84 mgN-NO_2^-/gVSS/h ($R^2 = 0,9$) and 299 mgS-HS^-/gVSS/h. NUR at FNA of 4–5 μgN/l was in fact comparable with the value observed in absence of nitrite. No clear nitrite consumption could be gauged from step2.

Summarising respirometric results, an average NUR of 90±10 mgN/gVSS/h was observed in all the tests, irrespective of nitrite or FNA concentration, whereas NiUR showed very sensitive to the applied conditions, ranging from 27 to 190 mgN/gVSS/h. The NUR value is in line with Manconi et al. (2007) and Mora et al. (2014), reporting specific NUR of 85 mgN/gVSS/h and 101±28 mgN/gVSS/h, respectively, for pure cultures of *T. denitrificans*. These figures are in agreement with other studies reporting that: (i) nitrite may be consumed at higher rates than nitrate when sulphide is used as e-donor, whereas the opposite is reported in case of sulphur as e-donor (Cui et al., 2019b; Sahinkaya et al., 2011); (ii) NO_2^-/FNA inhibition affects the denitritation step only, which is consistently modelled in many works according to Haldane-like kinetic for nitrite (Fajardo et al., 2014; Mora et al., 2015).

2. Conclusions

The promising results obtained in the present work are deemed relevant for gaining insight in the practical and theoretical framework of the novel PAD process. Influent S/N ratio below 0.8 gS/gN showed to be a sufficient control parameter in the highly SOB-enriched chemostat system, at low SRT (12–40 h). Nitrite Conversion Efficiency (NiCE) and Nitrite Accumulation Efficiencies (NiAE) achieved 73–95% and 60–70%, respectively, as average values over the three operational phases. The maximum NiCE of almost 100% was achieved at the lowest S/N ratio applied (0.58 gS/gN). Preliminary measurements on headspace N_2O warn about potentially significant emissions, calling for further monitoring studies. A clear population shift in microbial population from *Sulfurimonas* to *Thiobacillus* was observed after 80 days of strict and stable S-limiting operational conditions and suggests a possible role of growth bioenergetics on the microbial ecology. In the perspective of its full-scale implementation in synergy with the anammox process, a control system will be necessary in order to optimise the sulphide removal and nitrite supply according to anammox and SOB requirement and it is considered an interesting focus for future works.

Authors' contributions

C. Polizzi: Conceptualization, wet laboratory, Supervision, writing. **D. Gabriel**: Supervision, discussion, fund acquisition. **G. Munz**: Supervision, discussion, fund acquisition.

Declaration of competing interest

The authors declare that they have no known competing financial interests or personal relationships that could have appeared to influence the work reported in this paper.

Acknowledgements

The present work was supported by a financial contribution from Consorzio Cuoiodepur S.p.a. (Pisa, IT) and was partially developed within the Project Recycles (GA: 872053 funded by the European Commission within the Horizon 2020 Mary Sklodowska Curie Rise 2019 programme. The authors would like to thank professor Matteo Ramazzotti from the Department of Biomedical, Experimental and Clinical Sciences "Mario Serio" of the University of Florence for his support in NGS data handling.

Appendix A. Supplementary data

Supplementary data to this article can be found online at https://doi.org/10.1016/j.chemosphere.2022.133936.

References

Anthonisen, A.C., Loehr, R.C., Prakasam, T.B., Srinath, E.G., 1976. Inhibition of nitrification by ammonia and nitrous acid. J. Water Pollut. Control Fed. 48, 835–852.

APHA, 2005. APHA: Standard Methods for the Examination of Water and Wastewater, twenty-first ed. American Public Health Association/American Water Works Association/Water Environment Federation, Washington DC.

Campos, J.L., Carvalho, S., Portela, R., Me, R., 2008. Kinetics of denitrification using sulphur compounds : effects of S/N ratio. Endogen. Exogen. Comp. 99, 1293–1299. https://doi.org/10.1016/j.biortech.2007.02.007.

Can-dogan, E., Turker, M., Dagasan, L., Arslan, A., 2010. Sulfide removal from industrial wastewaters by lithotrophic denitrification using nitrate as an electron acceptor. Water Resour. Ind. 2286–2293. https://doi.org/10.2166/wst.2010.545.

Chen, F., Li, X., Gu, C., Huang, Y., Yuan, Y., 2018. Selectivity control of nitrite and nitrate with the reaction of S0 and achieved nitrite accumulation in the sulfur autotrophic denitrification process. Bioresour. Technol. 266, 211–219. https://doi.org/10.1016/j.biortech.2018.06.062.

Cheng, Y., Zhang, Y., Shen, Q., Gao, J., Zhuang, G., Zhuang, X., 2017. Effects of exogenous short-chain N-acyl homoserine lactone on denitrifying process of Paracoccus denitrificans. J. Environ. Sci. 54, 33–39. https://doi.org/10.1016/j.jes.2016.05.019.

Claus, G., Kutzner, H.J., 1985. Physiology and kinetics of autotrophic denitrification by Thiobacillus denitrificans. Appl. Microbiol. Biotechnol. 283–288.

Cristovao, R., Botelho, C., Martins, R., Loureiro, J.M., Boaventura, R.A.R., 2015. Fish canning industry wastewater treatment for water reuse e a case study. J. Clean. Prod. 87 https://doi.org/10.1016/j.jclepro.2014.10.076.

Cui, Y., Biswal, B.K., Guo, G., Deng, Y., Huang, H., 2019a. Biological nitrogen removal from wastewater using sulphur-driven autotrophic denitrification. Appl. Microbiol. Biotechnol. 6023–6039.

Cui, Y., Guo, G., Ekama, G.A., Deng, Y., Chui, H., Chen, G., Wu, D., 2019b. Elucidating the bio fi lm properties and biokinetics of a sulfur-oxidizing moving-bed bio fi lm for mainstream nitrogen removal. Water Res. 162, 246–257. https://doi.org/10.1016/j.watres.2019.02.061.

Dapena-mora, A., Fern, I., Campos, J.L., Mosquera-corral, A., Jetten, M.S.M., 2007. Evaluation of activity and inhibition effects on Anammox process by batch tests based on the nitrogen gas production. Enzym. Microb. Technol. 40 40, 859–865. https://doi.org/10.1016/j.enzmictec.2006.06.018.

Van Deng, Y., Ekama, G.A., Cui, Y., Tang, C., Loosdrecht, M.C.M., Chen, G., Wu, D., 2019. Coupling of Sulfur (Thiosulfate) -driven Denitratation and Anammox Process to Treat Nitrate and Ammonium Contained Wastewater 163. https://doi.org/10.1016/j.watres.2019.114854.

Van Deng, Y., Wu, D., Huang, H., Cui, Y., Loosdrecht, M.C.M., Chen, G., 2021. Exploration and verification of the feasibility of sulfide-driven partial denitrification coupled with anammox for wastewater treatment. Water Res. 193. https://doi.org/10.1016/j.watres.2021.116905.

Fajardo, C., Mora, M., Fernández, I., Mosquera-corral, A., Luis, J., Mendez, R., 2014. Chemosphere Cross effect of temperature , pH and free ammonia on autotrophic

denitrification process with sulphide as electron donor. Chemosphere 97, 10–15. https://doi.org/10.1016/j.chemosphere.2013.10.028.
Ghosh, W., Dam, B., 2009. Biochemistry and molecular biology of lithotrophic sulfur oxidation by taxonomically and ecologically diverse bacteria and archaea. FEMS Microbiol. Rev. https://doi.org/10.1111/j.1574-6976.2009.00187.x.
Glass, C., Silverstein, J., 1998. Denitrification kinetics OF high nitrate concentration water : pH effect on inhibition and nitrite accumulation. Water Res. 32, 831–839.
Huang, S., Yu, D., Chen, G., Wang, Y., Tang, P., 2021. Realization of nitrite accumulation in a sulfide-driven autotrophic denitri fi cation process : simultaneous nitrate and sulfur removal. Chemosphere 278, 130413. https://doi.org/10.1016/j.chemosphere.2021.130413.
Jain, M., Majumder, A., Sarathi, P., Kumar, A., 2020. A review on treatment of petroleum refinery and petrochemical plant wastewater : a special emphasis on constructed wetlands. J. Environ. Manag. 272, 111057. https://doi.org/10.1016/j.jenvman.2020.111057.
Kalyuzhnyi, S.V., Mulder, A., Consultancy, A.E., Versprille, B., 2006. New Anaerobic Process of Nitrogen Removal. https://doi.org/10.2166/wst.2006.729.
Klatt, J.M., Polerecky, L., 2015. Assessment of the stoichiometry and efficiency of CO 2 fixation coupled to reduced sulfur oxidation. Front. Microbiol. 6 https://doi.org/10.3389/fmicb.2015.00484.
Liu, C., Li, W., Li, X., Zhao, D., Ma, B., Wang, Y., Liu, F., Lee, D., 2017. Nitrite accumulation in continuous-flow partial autotrophic denitrification reactor using sulfide as electron donor. Bioresour. Technol. 243, 1237–1240. https://doi.org/10.1016/j.biortech.2017.07.030.
Liu, Y., Peng, L., Ngo, H.H., Guo, W., Wang, D., Pan, Y., Sun, J., Ni, B., 2016. Evaluation of nitrous oxide emission from sulfide- and sulfur-based autotrophic denitrification processes. Environ. Sci. Technol. https://doi.org/10.1021/acs.est.6b02202.
Manconi, I., Carucci, A., Lens, P., 2007. Combined removal of sulfur compounds and nitrate by autotrophic denitrification in bioaugmented activated sludge system. Biotechnol. Bioeng. 98, 551–560. https://doi.org/10.1002/bit.
Mannucci, A., Munz, G., Mori, G., Lubello, C., 2010. Anaerobic treatment of vegetable tannery wastewaters : a review. DES 264, 1–8. https://doi.org/10.1016/j.desal.2010.07.021.
Mora, M., 2014. Characterization of S-Oxidizing Biomass through Respirometric Techniques under Anoxic and Aerobic Conditions. Universitat Autonoma de Barcelona.
Mora, M., Fernández, M., Gómez, J.M., Cantero, D., Lafuente, J., Gamisans, X., 2015. Kinetic and Stoichiometric Characterization of Anoxic Sulfide Oxidation by SO-NR Mixed Cultures from Anoxic Biotrickling Filters 77–87. https://doi.org/10.1007/s00253-014-5688-5.
Mora, M., Guisasola, A., Gamisans, X., Gabriel, D., 2014. Examining thiosulfate-driven autotrophic denitrification through respirometry. Chemosphere 113, 1–8. https://doi.org/10.1016/j.chemosphere.2014.03.083.
Moraes, B.S., Foresti, E., 2012. Bioresource Technology Determination of the intrinsic kinetic parameters of sulfide-oxidizing autotrophic denitrification in differential reactors containing immobilized biomass. Bioresour. Technol. 104, 250–256. https://doi.org/10.1016/j.biortech.2011.11.050.
Mulder, A., Van De, Graaf A.A., Robertson, L.A., Kuenen, J.G., 1995. Anaerobic ammonium oxidation discovered in a denitrifying fluidized bed reactor. FEMS Microbiol. Ecol. 16, 177–184.
Oh, S., Kim, K., Choi, H., Cho, J., Kim, I.S., 2000. Kinetics and physiological characteristics of autotrophic dentrification by denitrifying sulfur bacteria. Water Sci. Technol. 59–68.
Russ, L., Speth, D.R., Jetten, M.S.M., Op den Camp, H.J.M., Kartal, B., 2014. Interactions between anaerobic ammonium and sulfur-oxidizing bacteria in a laboratory scale model system. Environ. Microbiol. 16, 3487–3498. https://doi.org/10.1111/1462-2920.12487.
Sahinkaya, E., Hasar, H., Kaksonen, A.H., Rittmann, B.E., 2011. Sahinkaya et al. 2011, Performance of a sulphide-oxidising, sulphur producing membrane biofilm reactor treating sulphide containing bioreactor effluent. Environ. Sci. Technol. 45, 4080–4087 pdf 4080–4087.
Sparacino-Watkins, C., Stolz, J.F., Basu, P., 2014. Nitrate and periplasmic nitrate reductases. Chem. Soc. Rev. 676–706. https://doi.org/10.1039/c3cs60249d.
Van Den Bosch, P.L.F., Van Beusekom, O.C., Buisman, C.J.N., Janssen, A.J.H., 2007. Sulfide oxidation at halo-alkaline conditions in a fed-batch bioreactor. Biotechnol. Bioeng. 97, 1053–1063. https://doi.org/10.1002/bit.
Wang, Y., Li, P., Zuo, J., Gong, Y., Wang, S., Shi, X., 2018. Inhibition by free nitrous acid (FNA) and the electron competition of nitrite in nitrous oxide (N 2 O) reduction during hydrogenotrophic denitri fi cation. Chemosphere 213, 1–10. https://doi.org/10.1016/j.chemosphere.2018.08.135.
Yang, W., Zhao, Q., Lu, H., Ding, Z., Meng, L., Chen, G., 2016. Sulfide-driven autotrophic denitri fi cation signi fi cantly reduces N2O emissions. Water Res. 90, 176–184. https://doi.org/10.1016/j.watres.2015.12.032.
Zhang, Z., Zhang, Y., Chen, Y., 2019. Recent advances in partial denitrification in biological nitrogen removal : from enrichment to application. Bioresour. Technol. 122444. https://doi.org/10.1016/j.biortech.2019.122444.
Zhou, Y., Oehmen, A., Lim, M., Vadivelu, V., Jern Ng, W., 2011. The role of nitrite and free nitrous acid (FNA) in wastewater treatment plants. Water Res. 5, 4672–4682. https://doi.org/10.1016/j.watres.2011.06.025.
Zhou, Y., Pijuan, M., Yuan, Z., 2007. Free nitrous acid inhibition on anoxic phosphorus uptake and denitrification by poly-phosphate accumulating organisms. Biotechnol. Bioeng. 98, 903–912. https://doi.org/10.1002/bit.